International Journal of Disaster Risk Science (2026) 17:161–181
https://doi.org/10.1007/s13753-026-00691-4

www.ijdrs.com
www.springer.com/13753

ARTICLE

Urban Flood Prediction Model Based on Explainable Deep Learning and Attention Mechanism

Shanlun Xu[1] · Huiliang Wang[1] · Hongshi Xu[1] · Zening Wu[1] · Xiangyang Zhang[1] · Yihong Zhou[1] · Wanjie Xue[1]

Accepted: 6 January 2026 / Published online: 20 January 2026

Abstract
Deep learning models are widely used for urban flood prediction, but current research lacks a clear explanation of how indicator weight changes affect model accuracy. This study incorporated the attention mechanism between the convolutional and fully connected layers of the convolutional neural network (CNN) to enable the model to focus on critical flood-inducing factors, and employed the particle swarm optimization (PSO) to optimize the key hyperparameters (for example, the number of filters and learning rate). Furthermore, we employed Shapley additive explanation (SHAP) to analyze how flood-inducing indicator weight changes affect prediction accuracy. The model was tested on Haidian Island, China. The Nash-Sutcliffe efficiency (NSE) coefficient of the CNN model is 0.9287. After incorporating the attention mechanism into the CNN and optimizing the hyperparameters using PSO, the NSE is improved to 0.9503. The model demonstrates higher accuracy in predicting larger inundations, with the NSE for the 100-year return-period flood reaching 0.9535, compared to 0.8341 for the 5-year return period. Interpretability analysis shows that elevation is the most important flood-inducing factor, accounting for 44% of the total importance, followed by tidal levels, which account for 33%. The attention mechanism increases the weights of important flood-inducing factors (for example, elevation, tide level); after hyperparameter optimization, the model achieves more comprehensive learning, increasing the weights of the rainfall indicators that are neglected by the unoptimized model, and these weight changes improve the accuracy of the model. The research revealed the impacts of different flood-inducing factors on flooding and the influence of indicator weight changes on model accuracy.

Keywords Attention mechanism · Change in indicator weights · Explainable deep learning · Particle swarm optimization · Urban flood

1 Introduction

Climate change has increased the frequency of extreme weather events (Zhang et al. 2024) that are marked by long durations, intense peaks, and heavy rainfall, leading to large-scale urban flooding (Cheng et al. 2025; Li et al. 2025). Rapid urbanization has altered surface conditions, reduced infiltration, and increased runoff, further aggravated flooding (Ma, Chen, et al. 2022; Mei et al. 2024). Recent disasters illustrate this trend: in July 2020, heavy rainfall in Japan caused widespread flooding, resulting in at least 80 deaths and tens of thousands displaced; in July 2021, Zhengzhou recorded 201.9 mm of rainfall within one hour, causing 380 deaths and USD 6.37 billion in economic losses (Wu et al. 2022); in September 2023, record-breaking rainfall totaling more than 600 mm hit Shenzhen, flooding 285 residential communities and 19,500 vehicles, with losses of about USD 170 million. Therefore, flood prediction and disaster prevention have become important research topics (Liu et al. 2024; Yang et al. 2024).

Deep learning models have been extensively applied across various fields for their ability to quickly and accurately solve prediction and classification problems (Yan et al. 2021). Specifically, in urban flood prediction, researchers have used models such as gradient boosting decision trees (GBDT) (Wang et al. 2023), convolutional neural network (CNN) (Kabir et al. 2020), and ensemble machine learning frameworks that combine XGBoost, multilayer perceptron

✉ Huiliang Wang
wanghuiliang@zzu.edu.cn

✉ Hongshi Xu
xuhongshi@zzu.edu.cn

[1] Yellow River Laboratory, School of Water Conservancy and Transportation, Zhengzhou University, Zhengzhou 450001, China

(MLP), and other deep learning models (Zhu et al. 2024) to forecast inundation and identify flood-prone areas. In developing urban flooding prediction models based on deep learning, the weights of flood-inducing factors are different. For instance, low elevation areas are more prone to flooding, while high tide level in coastal areas is a major flood-inducing factor. However, few studies have focused on enhancing the models' attention to important flood-inducing indicators while reducing the weight of less significant ones, thereby improving model predictive accuracy. Inspired by human cognitive processes, attention mechanisms enable models to concentrate on the most relevant portions of the input information (Brauwers and Frasincar 2023). Attention mechanisms do not treat all input features equally. Instead, they dynamically assign varying importance levels to different sections of the data, enabling more efficient and accurate predictions (Lv et al. 2022). At present, attention mechanisms are successfully applied in machine translation (Britz et al. 2017), action recognition (Liu et al. 2020), and other fields (Guo et al. 2023). Therefore, this study aimed to incorporate the attention mechanism into the deep learning model, thereby amplifying the influence of key flood-inducing factors and boosting prediction precision.

For enhancing the accuracy of deep learning models, many studies focused on optimizing model hyperparameters (Yang and Shami 2020; Ali et al. 2023). They commonly adopted hyperparameter optimization techniques, including the grid search (GS) algorithm (Pan et al. 2022), genetic algorithm (GA) (Bouktif et al. 2018), and Bayesian optimization (BO) (Wang et al. 2023). However, traditional methods often suffer from slow convergence or local optima issues. Particle swarm optimization (PSO)'s ability to balance global and local exploration allows it to avoid local optima and efficiently find global solutions (Xu et al. 2022). For example, PSO achieves optimization results that are comparable to those of GS, while consuming only 1% to 30% of the time required by GS (Ribalta et al. 2017). In the Rosenbrock function optimization, PSO achieved an average minimum of 0.00057 with fewer evaluations, outperforming GA (0.0014) (Tani et al. 2021). In the hydrological field, Xu et al. (2022) used PSO to optimize the hyperparameters in Long Short-Term Memory (LSTM), improving its Nash-Sutcliffe efficiency (NSE) from 0.8462 to 0.8869 in 6-hour runoff forecasting. In this study, PSO was used to optimize hyperparameters of the deep learning model, enhancing flood prediction accuracy.

Although some previous studies have explored the attention mechanism and hyperparameter optimization, the optimized models remain as "black-box" models, failing to explain why the models' accuracy have improved. Shapley additive explanation (SHAP) and Local Interpretable Model-agnostic Explanations (LIME) are currently two commonly used techniques in Explainable Artificial Intelligence (XAI). The LIME aims to explain a model's predictions by approximating it locally around a specific instance. Hemel and Sakib (2024) used LIME to analyze the relationship between rainfall and flooding under specific conditions in Bangladesh. However, the local explanations generated by LIME are specific to individual samples and lack a global perspective. Shapley value concept from cooperative game theory is used by SHAP for enabling interpretability analysis of deep learning models (Zhang et al. 2023). SHAP provides not only local explanations but also a quantitative and global approach to measure how different variables contribute to both individual predictions and the overall model outcomes. It has been used in the area of water conservancy (Wang et al. 2024), such as runoff prediction (Yao et al. 2023), water quality prediction (Park et al. 2022), and urban flood prediction (Gao et al. 2024). For instance, Gao et al. (2024) used the CNN model for predicting urban flood, and then SHAP was adopted to analyze the connection between input indicators and inundation depth. But few studies used SHAP to explain which indicators' weights increase after incorporating the attention mechanism in deep learning-based urban flood model, and how hyperparameter optimization improves the model's accuracy.

Data-driven models have made some progress in urban flood prediction, but current research lacks a clear explanation of how indicator weight changes affect model accuracy. In this study, the attention mechanism was added to CNN to increase the weights of important flood-inducing indicators in the model, thereby improving the prediction accuracy. Unlike conventional channel-wise or spatial attention mechanisms, this study designed an additive attention module to directly learn the relative importance of flood-inducing factors along the convolutional features. This structure focuses on indicator-level relevance, rather than feature-map correlations, which better aligns with the identification of the relative importance of different flood-inducing factors. The attention mechanism enhances the model's focus on key flood-inducing factors, PSO ensures efficient and globally convergent hyperparameter optimization, and SHAP explains how the changes in the weights of flood-inducing factors, resulting from the incorporation of the attention mechanism and hyperparameter optimization, affect the model's prediction accuracy.

Therefore, our study proposed an interpretable urban flood prediction model based on attention mechanism-deep learning model. The major contributions lie in the following aspects: (1) Incorporating the attention mechanism enables the deep learning model to increase the weights of important flood-inducing factors, allowing for more accurate predictions of urban inundation. (2) The SHAP approach is employed to analyze how changes in the weights of flood-inducing indicators affect prediction accuracy. The rest of the article is organized as follows: Section 2 presents the

framework and methods. Section 3 contains study area and data. Section 4 presents results and discussion. Section 5 describes the conclusion.

2 Methodology

This study developed an urban flood prediction model based on explainable deep learning model and the attention mechanism. Figure 1 demonstrates the flow of model construction: (1) Develop a physical model of urban flooding based on Personal Computer Storm Water Management Model (PCSWMM), which is used for simulating inundation depths under various conditions. ArcGIS is used to extract disaster-breeding environment data of the study area. (2) The combination of rainfall data, tide level data, disaster-breeding environment data, and inundation depth data provides the data basis for the deep learning model. The urban flood prediction model is constructed by employing CNN. Incorporating the attention mechanism allows the model to emphasize critical input variables, and the hyperparameters are optimized by using PSO. Assessing the model's performance, and the model accuracies of CNN, attention mechanism-convolutional neural network (AM-CNN) and particle swarm optimization-attention mechanism-convolutional neural network (PSO-AM-CNN) are compared. (3) Shapley additive explanation is employed to explain the importance of different flood-inducing factors in the model, while also revealing the impact of indicator weight changes on model accuracy.

2.1 Physical Model of Urban Flooding

The PCSWMM is widely applied in environmental engineering, water resource management, and urban flooding simulation (Ma, Wu, et al. 2022). It supports comprehensive analyses of storm runoff and urban inundation under various scenarios, aiding the design of effective drainage and flood management systems. The model couples a 1D hydrodynamic pipeline module based on pipe network data with a 2D surface inundation module derived from elevation data (Manchikatla and Umamahesh 2022).

During rainfall events, water enters the pipe network through inspection wells and is routed using the dynamic wave method in the 1D module. When the drainage capacity is exceeded and overflow occurs, the 2D surface module computes the overland flow. The surface of the study area is discretized into hexagonal or rectangular grids, each represented by a 2D inspection node that records essential attributes, enabling accurate simulation of surface water movement across regions.

2.2 Convolutional Neural Network

Convolutional neural network is a remarkable innovation in the field of artificial intelligence. This neural network utilizes a multilayered structure and convolutional techniques (Kang et al. 2025). Modern convolutional neural networks originated from LeNet networks (LeCun et al. 1989). The success of LeNet demonstrated the potential of CNN for practical applications and paved the way for further research and development in deep learning, ultimately leading to the widespread adoption of CNN in various artificial intelligence domains.

Compared with traditional machine learning models, CNNs are more scalable and effective for large, complex datasets. Their efficiency arises from two key principles: local receptive fields, which capture spatial or sequential dependencies, and weight sharing, which reduces parameters and mitigates overfitting. 1D-CNN can effectively extract temporal or sequential features from data and has been successfully applied to flood prediction (Gao et al. 2024). Therefore, this study employs a 1D-CNN to predict inundation depth in the study area.

2.3 Attention Mechanism

In deep learning, the attention mechanism is understood as a method of filtering out key information from a plenty of input data and focusing more attention on these crucial pieces of information in order to make effective decisions (Niu et al. 2021). The process of focusing is generally achieved by calculating weight coefficients for each position by the attention model, where larger values indicate greater focus on the corresponding information (Lv et al. 2022).

Attention could be understood as calculating a weighted sum of values using a query and associated keys. In this process, the query (Q), key (K), and value (V) are matrices, where the query determines which values should be prioritized based on their relevance to the keys (Alizadeh et al. 2021).

$$Attention\ Scores = \frac{QK^T}{\sqrt{d_k}} \tag{1}$$

where Q is the query matrix, K is the key matrix, d_k is the dimension of the keys, and K^T is the transpose of the key matrix. The term $\sqrt{d_k}$ in the denominator is used for maintaining gradient stability.

$$Attention\ Weights = Softmax\left(\frac{QK^T}{\sqrt{d_k}}\right) \tag{2}$$

The *Softmax* function converts the attention scores into weights that sum to 1, indicating the relative importance of each key in the context of the query.

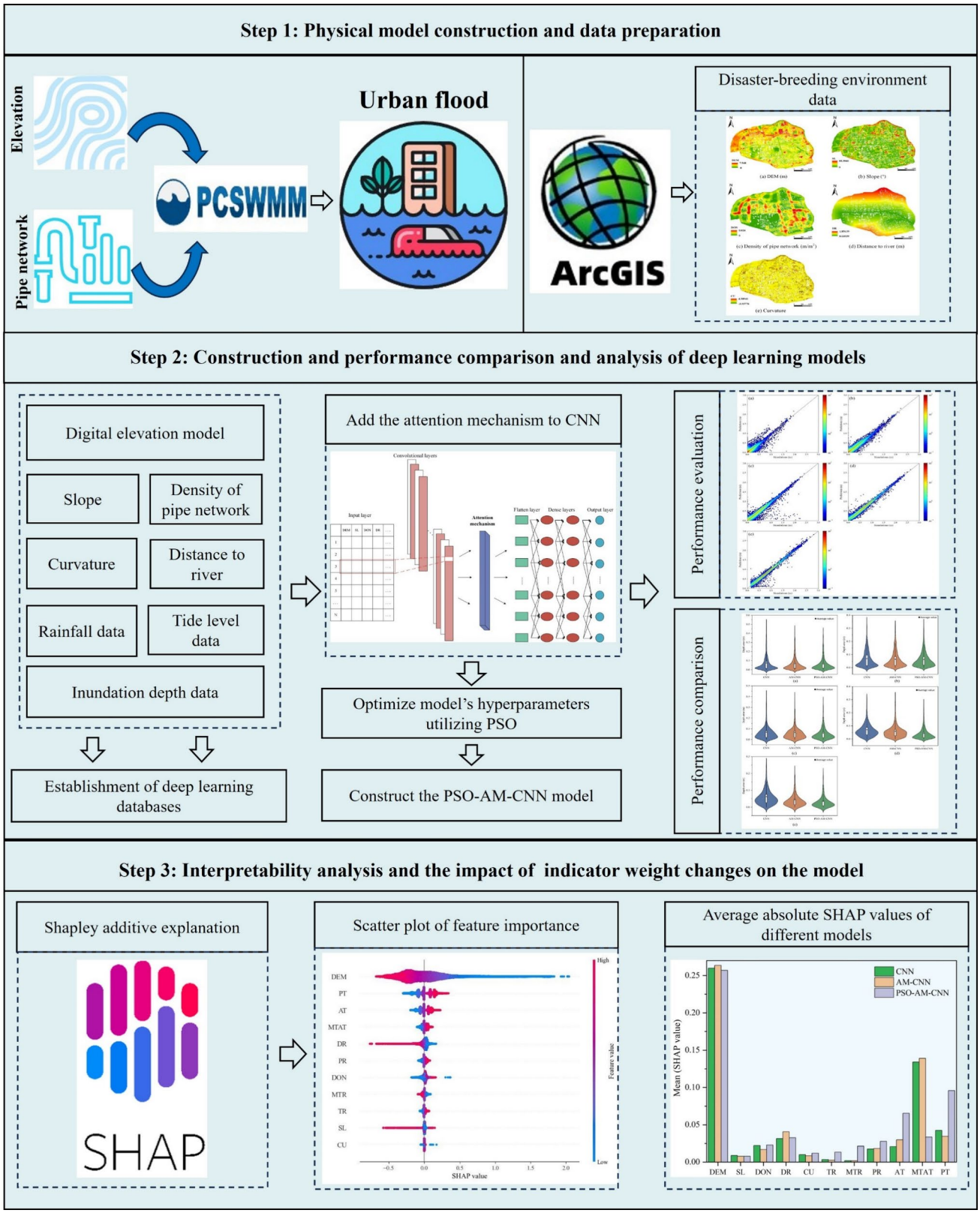

Fig. 1 Flowchart of the proposed interpretable urban flood prediction model based on attention mechanism-deep learning model

$$Attention(Q,K,V) = Softmax\left(\frac{QK^T}{\sqrt{d_k}}\right)V \tag{3}$$

where V is the value matrix. The final attention output is the sum of the values weighted, and the weights are derived from the attention mechanism.

2.4 Particle Swarm Optimization

Particle swarm optimization is an optimization algorithm inspired by the collective behavior of bird flocks and fish schools (Xu et al. 2022). It employs a swarm of particles, where each particle represents a candidate solution that explores the search space by updating its position based on its own best experience and the swarm's global best (Tang et al. 2021). Owing to its simplicity and efficiency, PSO is well suited for solving complex, high-dimensional optimization problems.

The velocity and position of each particle are updated as follows:

$$v_i(t+1) = wv_i(t) + c_1r_1\left(pBest_i - x_i(t)\right) + c_2r_2\left(gBest - x_i(t)\right) \tag{4}$$

$$x_i(t+1) = x_i(t) + v_i(t+1) \tag{5}$$

where $v_i(t)$ represents velocity of particle i at iteration t, $pBest_i$ and $gBest$ are the particle's personal best and the swarm's global best positions, w is inertia weight that manages the momentum of particle movement, c_1 and c_2 are the cognitive and social coefficients, $r_1, r_2 \in [0,1]$ are random numbers introducing stochasticity.

At each iteration, personal and global bests are updated based on fitness evaluation, and the process continues until a stopping criterion is met.

2.5 Model Performance Evaluation

For evaluating the model's performance, mean absolute error (MAE), root mean square error (RMSE), and Nash-Sutcliffe efficiency (NSE) (Nash and Sutcliffe 1970) are utilized. Low values of MAE and RMSE, along with a high NSE score indicate strong model performance. The formulas for these metrics are as follows:

$$MAE = \frac{1}{n}\sum_{i=1}^{n}|o_i - p_i| \tag{6}$$

$$RMSE = \sqrt{\frac{1}{n}\sum_{i=1}^{n}\left(\mathrm{o_i} - \mathrm{p_i}\right)^2} \tag{7}$$

$$NSE = 1 - \frac{\sum_{i=1}^{n}\left(\mathrm{o_i} - \mathrm{p_i}\right)^2}{\sum_{i=1}^{n}\left(\mathrm{o_i} - \mathrm{o}_{mean}\right)^2} \tag{8}$$

where n is sample size,o_i is the observed value, p_i is the predicted value, and o_{mean} is the average value of the observed value.

2.6 Explainability Method

Interpretability of deep learning models refers to their ability to clarify the reasoning behind predictions and identify influential factors. It enhances transparency and supports model optimization. Shapley additive explanation is an advanced interpretability approach based on Shapley values, originally introduced in cooperative game theory to allocate each participant's contribution to the overall outcome (Lundberg and Lee 2017; Wu et al. 2024). In deep learning, SHAP extends this concept by calculating the marginal contribution of each feature across all possible feature subsets, thereby quantifying its impact on model output.

Shapley additive explanation enables global interpretability by revealing features that most influence predictions and is widely applied to complex models such as ensembles and neural networks (Gao et al. 2024). The SHAP value for feature i is computed as follows (Pradhan et al. 2023):

$$\varphi_i = \sum_{S\in F\setminus\{i\}}\frac{|S|!(M-|S|!-1)!}{M!}\left[z_x(S\cup\{i\}) - z_x(S)\right] \tag{9}$$

where S represents a subset of the feature set F, M denotes total number of features, φ_i is the uniform metric of the additive feature attribute and is the SHAP value.

In this study, a larger absolute SHAP value indicates a stronger influence of that indicator on the predicted flood depth. When the model is optimized (for example, by PSO or attention mechanisms), internal feature weighting is adjusted, leading to redistribution of SHAP values among indicators. By comparing the mean absolute SHAP values before and after optimization, we can quantify how changes in feature importance correspond to observed improvements in accuracy metrics such as RMSE and NSE.

3 Case Study

This section introduces the primary situation of the study area and the basic data used in the research.

3.1 Study Area

Haidian Island is situated in the north of Haikou City, Hainan Province, China. Its total area is approximately 13.8 km^2. Figure 2 illustrates the location and topography of Haidian Island. Surrounded by water on all sides, its western and northern edges are adjacent to the Qiongzhou Strait, while its southern side is separated from the main island

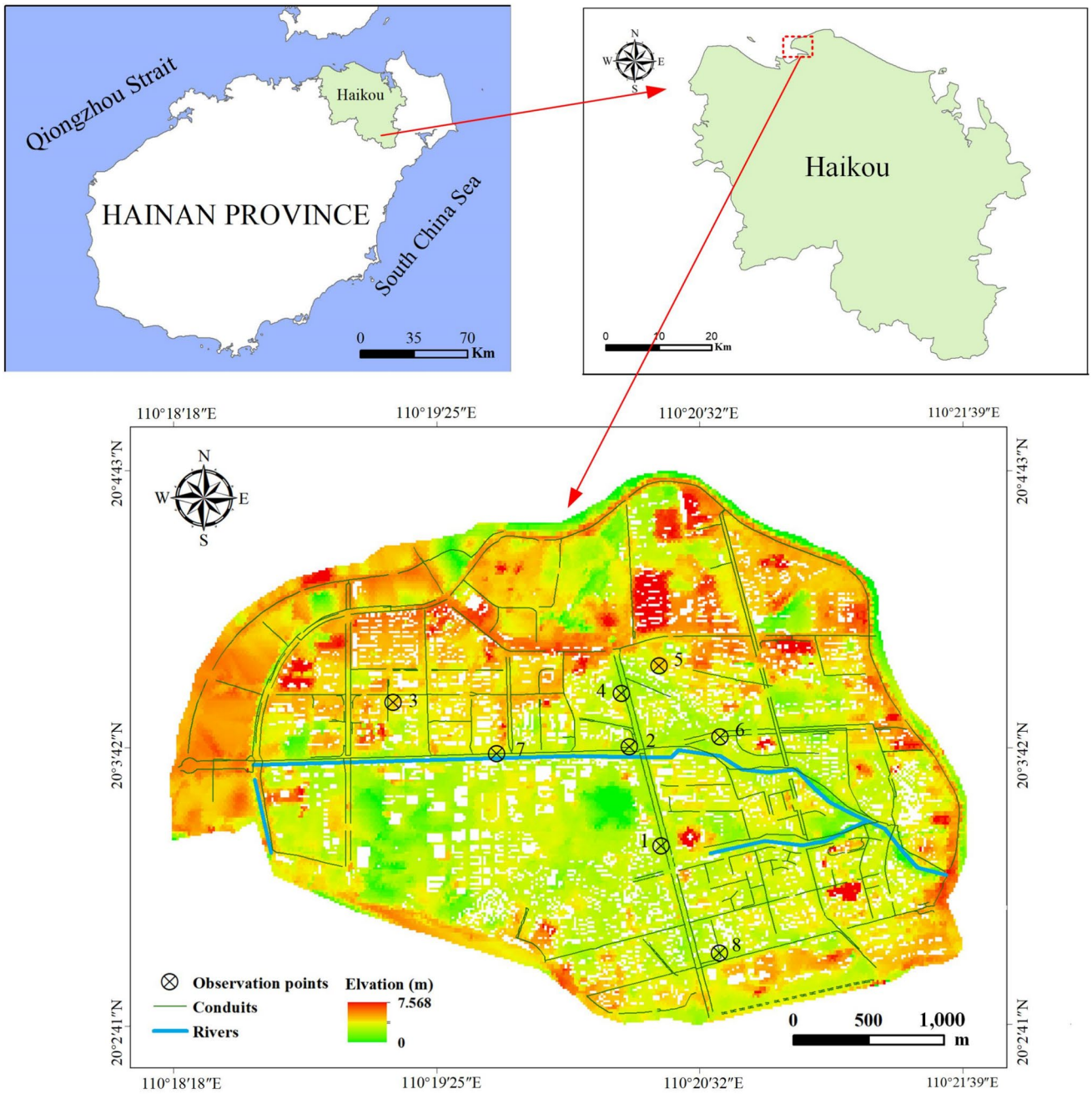

Fig. 2 Location of Haidian Island

of Hainan by Haidian Creek. Influenced by the monsoon climate, the study area experiences a high annual average rainfall (Xu et al. 2023), 78.1% of which falls during the rainy season. Haidian Island has a relatively flat terrain, and its aging drainage network makes the area highly susceptible to urban flooding, particularly under the joint impacts of heavy rainfall and tidal backflow. For instance, from 17 to 19 July 2014, Typhoon Rammasun hit Haikou, bringing a daily rainfall of up to 509.2 mm (Xu et al. 2018), and the resulting disaster affected 855,900 people, caused direct economic losses amounting to approximately USD 1.91 billion.

3.2 Data

In order to construct and validate the one-and two-dimensional (1D-2D) coupled physical model of urban flooding based on PCSWMM, the following data in the study area are required:

(1) Digital elevation model (DEM): DEM data serve as both the foundational data for constructing the 1D-2D model and a crucial indicator of disaster-breeding environment. Low-lying regions tend to accumulate water, increasing the risk of flooding. The DEM data are provided by the Institute of Geographic Sciences and Natural Resources Research at the Chinese Academy of Sciences. Using the ArcGIS software to process DEM (m), raster data with a spatial resolution of 25 m × 25 m are obtained.

(2) Pipe network data and river data: The pipe network data consist of one-dimensional pipes and monitoring wells. The one-dimensional pipes represent the urban drainage system, which includes rainwater and sewage pipes, among others. The detection wells are used to monitor water level and flow rate. River network data primarily include channel roughness and cross-sectional shapes of the rivers. Channel roughness indicates the resistance faced by water flow in the river, while the cross-sectional shape influences the flow pattern of the water. These datasets are provided by the Haikou Water Bureau.

(3) Historical rainfall and tide level data, observed inundation depth data: The historical rainfall and tide level data include daily maximum rainfall and daily maximum tide levels from 1970 to 2013, as well as the rainfall and tide level process data during Typhoon Rammasun in 2014. We removed outliers in historical time series data and performed interpolation to ensure the continuity and completeness of the data. Observed inundation depth data include the locations of observation points (see Fig. 2) and inundation depths. These datasets are provided by the Haikou Water Bureau.

In order to establish an urban flood prediction model based on deep learning, disaster-breeding environment data are the important input variables. In addition to elevation, the following variables were selected as disaster-breeding environment factors. Figure 3 presents the data of these variables processed by ArcGIS.

(1) Slope: Slope represents inclination degree of the Earth's surface. In areas with a gentle slope, the flow velocity of surface runoff is relatively slow, and the flood generated by rainfall gathers, which is difficult to quickly drain away.
(2) Density of pipe network: Areas with lower pipe network density may experience difficulties in timely water discharge, potentially leading to waterlogging.
(3) Distance to river: The data quantify the distance from the grids to the closest river nearby. Areas closer to rivers face a higher flood risk due to the potential for levee overtopping, whereas areas farther away are generally less vulnerable.
(4) Curvature: Curvature describes the rate of change of the slope. A negative curvature indicates a concave surface, where water tends to converge. Conversely, a positive curvature indicates a convex surface, where water tends to diverge.

Disaster-breeding environment factors (DEM, slope, density of pipe network, distance to river, and curvature) are uniformly resampled to a spatial resolution of 25 m × 25 m, outliers are removed, and min-max normalization is applied to scale the values to a 0–1 range.

4 Results and Discussion

This section presents the core results to verify the model's effectiveness, including PCSWMM physical model validation, deep learning dataset preparation, deep learning model construction, hyperparameter optimization using PSO, model performance evaluation, and interpretability analysis using SHAP.

4.1 Construction and Verification of the Physical Model of Urban Flooding

The ArcGIS software was employed to process the drainage pipe network and 1D inspection well data, with the original pipe network simplified. The 1D inspection wells and pipe network are presented in Fig. 4a. Based on the topography and geomorphology characteristics, current drainage pipes, and road layout, the study area is segmented into several sub-catchments, as illustrated in Fig. 4b.

The Manning's roughness coefficients for impervious and pervious areas are 0.02 and 0.2, respectively, while the pipe roughness coefficient is 0.01. Sub-catchments are delineated based on topographic slope (ranging from 0.55 to 0.855%) and flow accumulation, with areas varying from 35.97 to 210.12 ha. The urban flood simulation model consists of 2,042 1D pipelines, 13 sub-catchments, and 23,580 2D grids. To facilitate interaction between the 1D hydrodynamic pipe model and the 2D surface inundation model, the 1D-2D model adopts orifice connection approach.

To ensure the precision of the physical model of urban flooding, the rainfall and tide level data from Typhoon Rammasun on 18 July 2014 (Fig. 5) were employed as inputs for model calibration. Table 1 provides a detailed comparison of the simulated and observed maximum inundation depths. The absolute error between the observed and simulated depths remains below 0.1 m, with R^2 of 0.725, suggesting that the result is reliable (Xu et al. 2018). Thus, the simulation outcomes from the physical model based on PCSWMM are in close agreement with real-world scenarios, confirming the constructed model's accuracy.

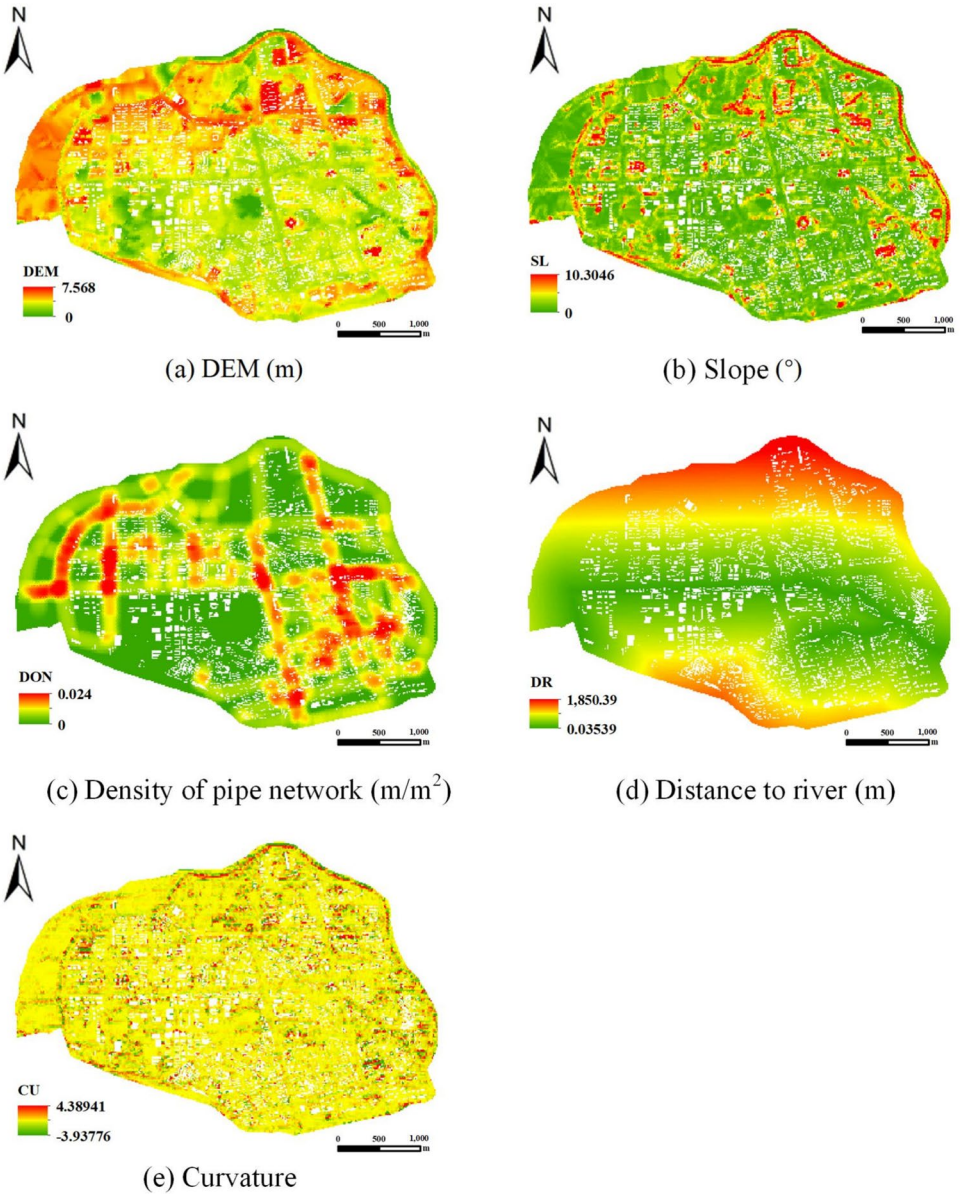

Fig. 3 Disaster-breeding environment factors in Haidian Island

4.2 Data Preparation

The deep learning model demands a substantial volume of training data. Rainfall and tide level data for various recurrence periods are determined by employing the generalized extreme value (GEV) function (Xu et al. 2020, Xue et al. 2024). Parameters of the GEV function for rainfall and tide level are calculated via maximum likelihood estimation (MLE) using the long-term historical series of daily maximum rainfall and daily maximum tide level in Haidian Island (1970–2013) (Xu et al. 2020). The parameters of GEV function are presented in Table 2. Taking the rainfall and tide level processes observed on 18 July 2014 as the typical event, we derive the design rainfall and tide level series for the 5, 10, 20, 50, and 100 years recurrence periods via the same ratio scaling method (Figs. 6 and 7). These design rainfall and tide level datasets corresponding to different recurrence periods are then paired to generate 25 rainfall-tide level events (a 5-year design rainfall and 5-year design tide level event, for example, is named R5-T5). The rainfall and tide level data are input into the PCSWMM model on an hourly basis to ensure the continuity of the time series.

Based on Wang et al. (2023), a grid is defined as susceptible to flood if the water depth surpasses 0.15 m. To reduce the interference of grids that are not affected by floods, only grids whose inundation depth is greater than 0.15 m in the extreme case (R100-T100) are regarded as the target grids of this study. Figure 8 illustrates the inundation conditions under R100-T100, and the statistical analysis shows that 13,157 grids have an inundation depth exceeding 0.15 m.

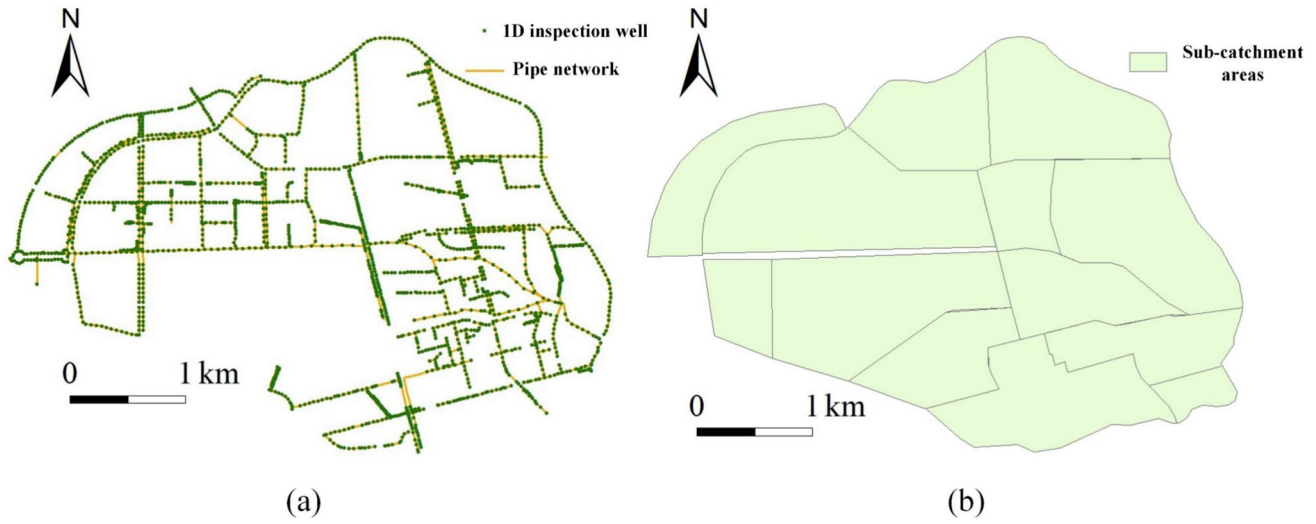

Fig. 4 The 1D pipe network **a** and sub-catchments **b** in Haidian Island

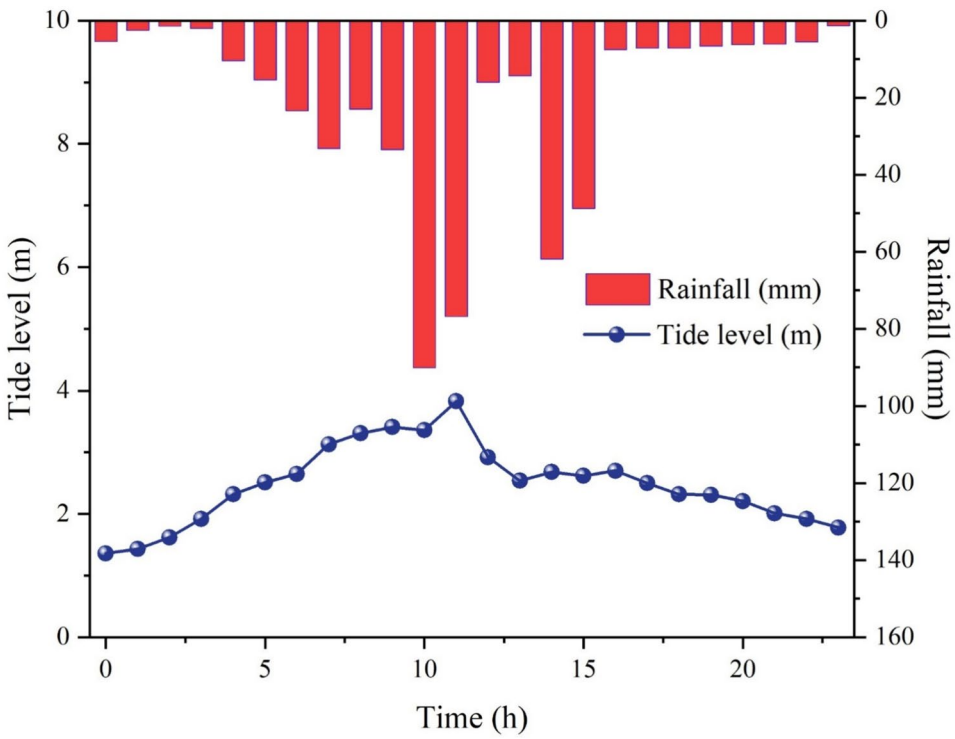

Fig. 5 Rainfall and tide level process on 18 July 2014

Therefore, there is a total of 328,925 simulated inundation depths under 25 events. The integration of rainfall, tide level, disaster-breeding environment, and inundation depth data forms the foundation for training the deep learning model.

The dataset is divided into training and testing sets in a ratio of 8:2, with a fixed random seed (seed = 42) to ensure experimental reproducibility. To demonstrate the model's prediction accuracy under different rainfall and tide level conditions, inundation depth under R5-T5, R10-T10, R20-T20, R50-T50, and R100-T100 are assigned to the test set, while inundation depth under the other conditions are divided into the training set.

4.3 Development of the Deep Learning Model and Hyperparameter Optimization

This section builds the AM-CNN model (by adding the attention mechanism to CNN) and uses PSO to optimize

Table 1 Error of the simulated depths as compared to the observed values

Observation points	Observed depth (m)	Simulated depth (m)	Absolute error (m)	Relative error (%)
1	0.40	0.43	0.03	7.50
2	0.60	0.55	−0.05	−8.33
3	0.55	0.54	−0.01	−1.82
4	0.45	0.42	−0.03	−6.67
5	0.60	0.58	−0.02	3.33
6	0.60	0.61	0.01	1.67
7	0.45	0.38	−0.07	−15.56
8	0.45	0.51	0.06	13.33

Table 2 Parameters of the generalized extreme value (GEV) function for rainfall and tide level

Parameters of GEV Function	Rainfall Distribution	Tide Level Distribution
Location parameter	122.51	2.349
Scale parameter	46.78	0.380
Shape parameter	0.115	−0.048

key hyperparameters (for example, number of filters, learning rate) for better prediction accuracy.

4.3.1 Construction of the Flood Prediction Model Based on Attention Mechanism-Convolutional Neural Network

This study uses the CNN to predict the inundation depth of Haidian Island. The model is developed using the Keras 2.12 module within TensorFlow 2.12 under the Python 3.10 environment. The Adam optimizer is adopted due to its relative low sensitivity to initial values of hyperparameters, which enhances the stability and reliability of model training. The mean squared error (MSE) is selected as the loss function because it penalizes large deviations in continuous flood depth prediction. Dropout is adopted to prevent model overfitting and enhance robustness. The initial 1D-CNN constructed in this study consists of 1 convolutional layer and 2 dense layers. In the convolutional layer, the number of filters is 64, the convolution kernel size is 2, and the first dense layer contains 50 neurons.

The selection of input indicators significantly impacts the predictive performance of deep learning models. Considering the topographic conditions and geographical location of Haidian Island, in addition to the disaster-breeding environment indicators and rainfall indicators considered in most studies, tide level is also an important disaster-causing

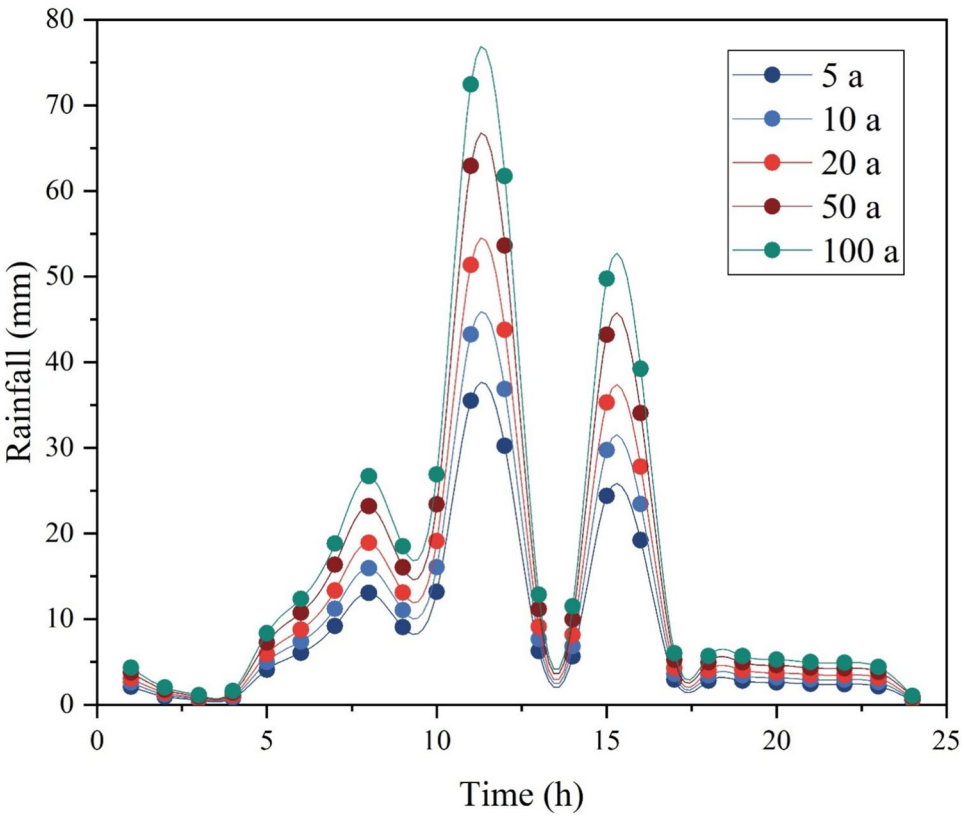

Fig. 6 Designed rainfall under different recurrence periods

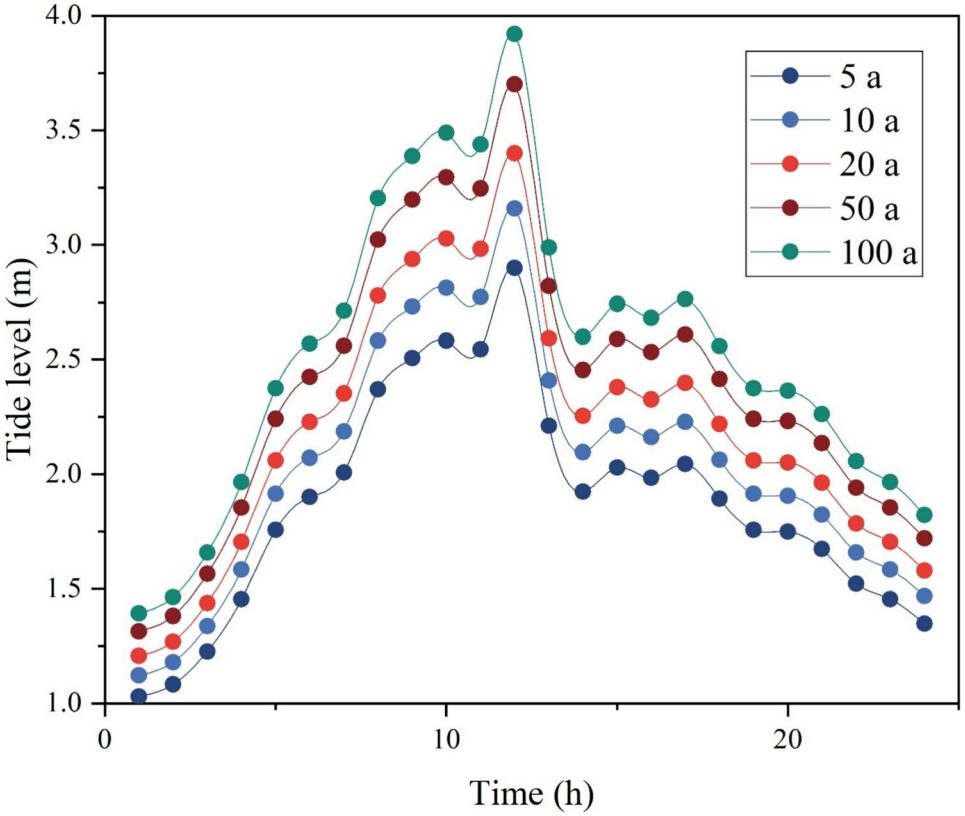

Fig. 7 Designed tide level under different recurrence periods

factor in this study. Table 3 illustrates the input and output indicators of CNN.

The attention mechanism is designed to allow the model to emphasize the most critical parts of the input data, enhancing overall performance. In urban flood applications, some areas are prone to flooding due to low-lying terrain, while coastal regions may experience flooding primarily due to elevated tide level. The attention mechanism makes the model prioritize variables that are more likely to cause flood, increasing the weight of important flood-inducing indicators. This study incorporates the attention mechanism between the convolutional layers and the dense layers, and Fig. 9 displays the simple structure of AM-CNN.

4.3.2 Particle Swarm Optimization for Hyperparameters

The CNN model involves many hyperparameters, among which five key hyperparameters—number of filters, kernel_size, neurons, learning_rate, and epochs—are selected for optimization due to their significant influence on the model. The five hyperparameters are configured within specific ranges based on experience and prior research (Kabir et al. 2020), with these ranges detailed in Table 4. The study employs ten-fold cross-validation (Bass and Bedient 2018) to assess model performance during training, using RMSE as the metric to evaluate the cross-validation results. Particle swarm optimization is implemented by employing the pyswarms library in Python 3.10 environment.

To obtain satisfactory hyperparameter optimization results quickly, the number of particles is configured as 100 iterations, the inertial weight w is 0.7, the sum of learning factors c_1 is 1.5, and the sum of learning factors c_2 is 2. The result of hyperparameter optimization using PSO is shown in Table 4. For the optimized hyperparameters, the minimum average RMSE achieved is 0.0958.

4.4 Performance Evaluation of the Particle Swarm Optimization-Attention Mechanism-Convolutional Neural Network (PSO-AM-CNN) Model

A comparison of inundation depth predicted by PSO-AM-CNN and the inundation depth simulated by PCSWMM in the test set is presented in Figs. 10a to e. In the 2D histograms, the diagonal represents perfect agreement between the predicted and simulated inundation depths, where points closer to the diagonal indicate more accurate predictions. In addition, the color intensity reflects point density, with darker shades signifying higher concentrations. Based on the figure, most points in the test set have good prediction performance. Under R5-T5, R10-T10, and R20-T20, many points exhibit small errors. Under R50-T50 and R100-T100,

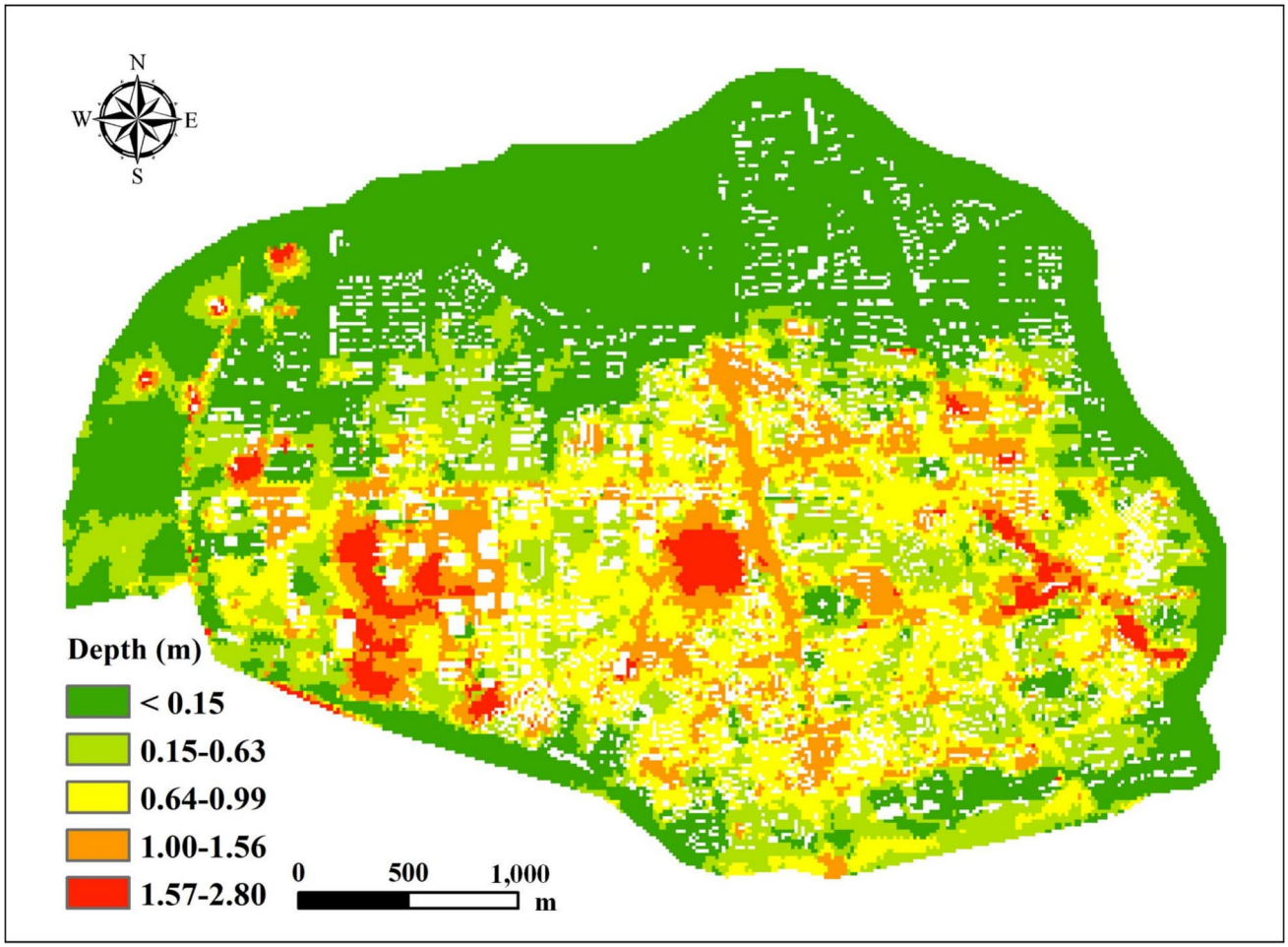

Fig. 8 Inundation conditions under R100-T100

Table 3 Input and output variables of the convolutional neural network (CNN)

Input variables	Disaster-breeding environment indicators	Rainfall indicators	Tide level indicators
	Digital elevation model (DEM)	Total rainfall (TR)	Peak tide level (PT)
	Density of pipe network (DON)	Peak rainfall (PR)	Average tide level (AT)
	Curvature (CU)	Maximum three-hour rainfall (MTR)	Maximum three-hour average tide level (MTAT)
	Distance to river (DR)		
	Slope (SL)		
Output variable	Maximum inundation depth		

although few points deviate significantly, more points are closer to the diagonal. The result shows that the model has better accuracy in predicting floods at high rainfall-tide levels.

The MAE, RMSE, and NSE are used to evaluate the PSO-AM-CNN model's performance. Figure 11 shows the trend of the MAE, RMSE, and NSE values for flood prediction across different return periods. In general, with the increase of return period, both the MAE and RMSE gradually decrease, while the NSE rises, indicating that the model achieves higher accuracy in simulating flood events under more extreme conditions. The NSE for the 100-year return-period flood reaching 0.9535, compared to 0.8341 for the 5-year return period. Then, we calculated the overall MAE, RMSE, and NSE of the model in the test set, which are 0.0528, 0.0973, and 0.9503 respectively. The MAE and RMSE are small, and the NSE is high, which indicates that the constructed model has high accuracy. The model achieved an NSE of 0.9503, which exceeds the performance of similar studies—for example, Yan et al. (2021) used the Elman neural network to predict flooding in Tianjin, with an NSE of 0.876; Huang et al. (2024) used the CNN-LSTM

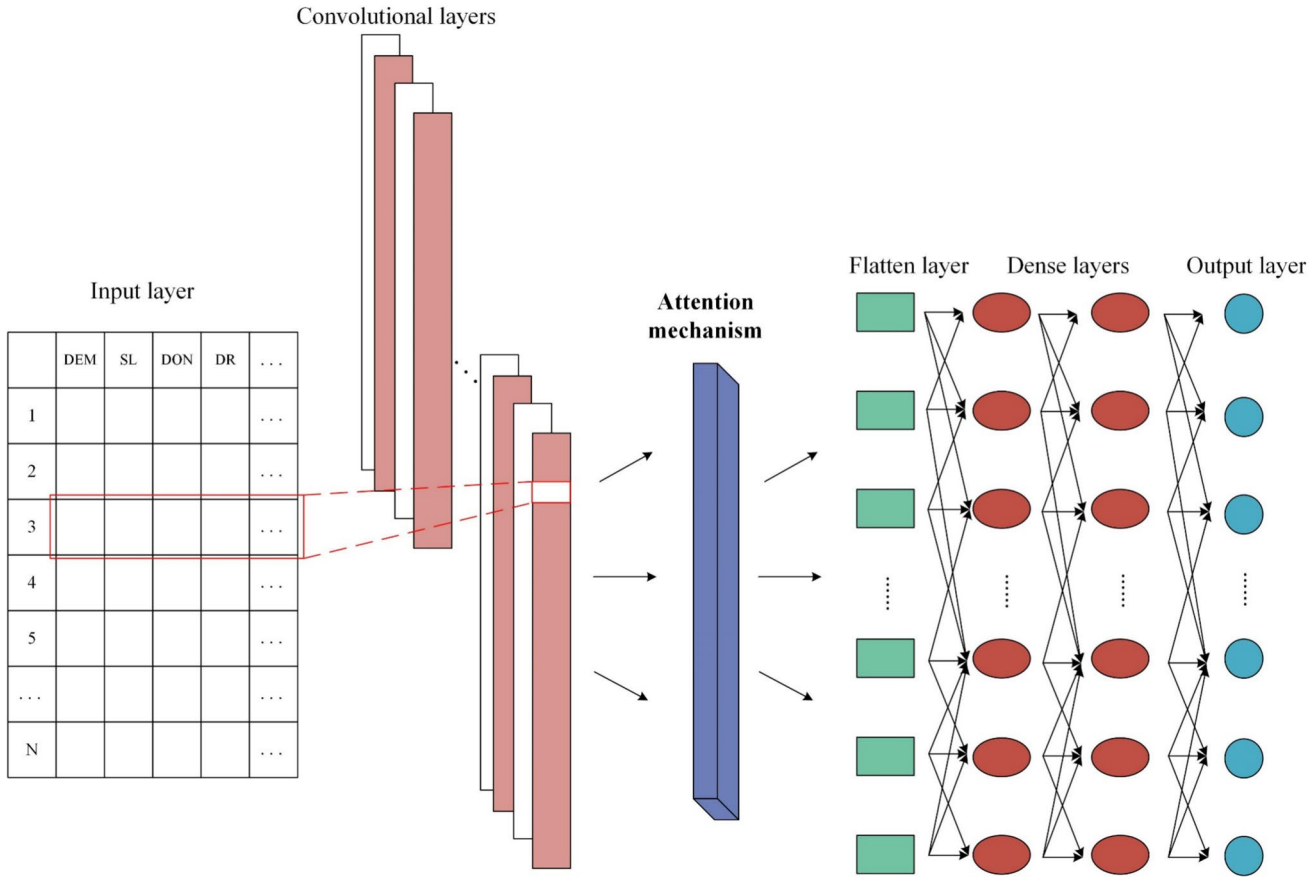

Fig. 9 A diagram of the attention mechanism-convolutional neural network (AM-CNN) model

Table 4 Optimization ranges of hyperparameters and optimization result

Hyperparameter	Minimum value	Maximum value	Optimization result
Number of filters	32	128	111
Kernel_size	2	5	3
Neurons	50	150	80
Learning_rate	0.001	0.01	0.0012
Epochs	10	100	80

model to predict flooding in the Beijiang River Basin in China, with an NSE of 0.838.

We used the same computer to test the average simulation times for the PSO-AM-CNN model and the PCSWMM model when simulating an urban flood scenario. The computer is equipped with an AMD Ryzen 7 7735H CPU (8 cores, 16 GB RAM) and an NVIDIA GeForce RTX 4050 GPU, running on the Windows 11 (64-bit) operating system. The PSO-AM-CNN model takes only 55 seconds on average, which is significantly faster than the 80 minutes required by the PCSWMM model. This substantial reduction in computation time highlights the proposed model's suitability for rapid urban flood prediction.

4.5 Comparison of the Convolutional Neural Network (CNN), Attention Mechanism-CNN (AM-CNN), and Particle Swarm Optimization-AM-CNN (PSO-AM-CNN) Models

To demonstrate the improvement in model accuracy achieved through incorporating the attention mechanism and hyperparameter optimization, we conducted an accuracy comparison between the PSO-AM-CNN, AM-CNN, and CNN models. Table 5 presents the performance of the CNN, AM-CNN, and PSO-AM-CNN models. The MAE and RMSE decreased across the CNN, AM-CNN, and PSO-AM-CNN models. The NSE of the CNN model with attention mechanism increased from 0.9287 to 0.9418, and the NSE increased to 0.9503 after hyperparameter optimization. This demonstrates that the approach used of the study significantly enhances the accuracy of urban flood prediction models.

Figure 12 demonstrates the inundation depth errors predicted by the CNN, AM-CNN, and PSO-AM-CNN models under different conditions in the test set. When compared

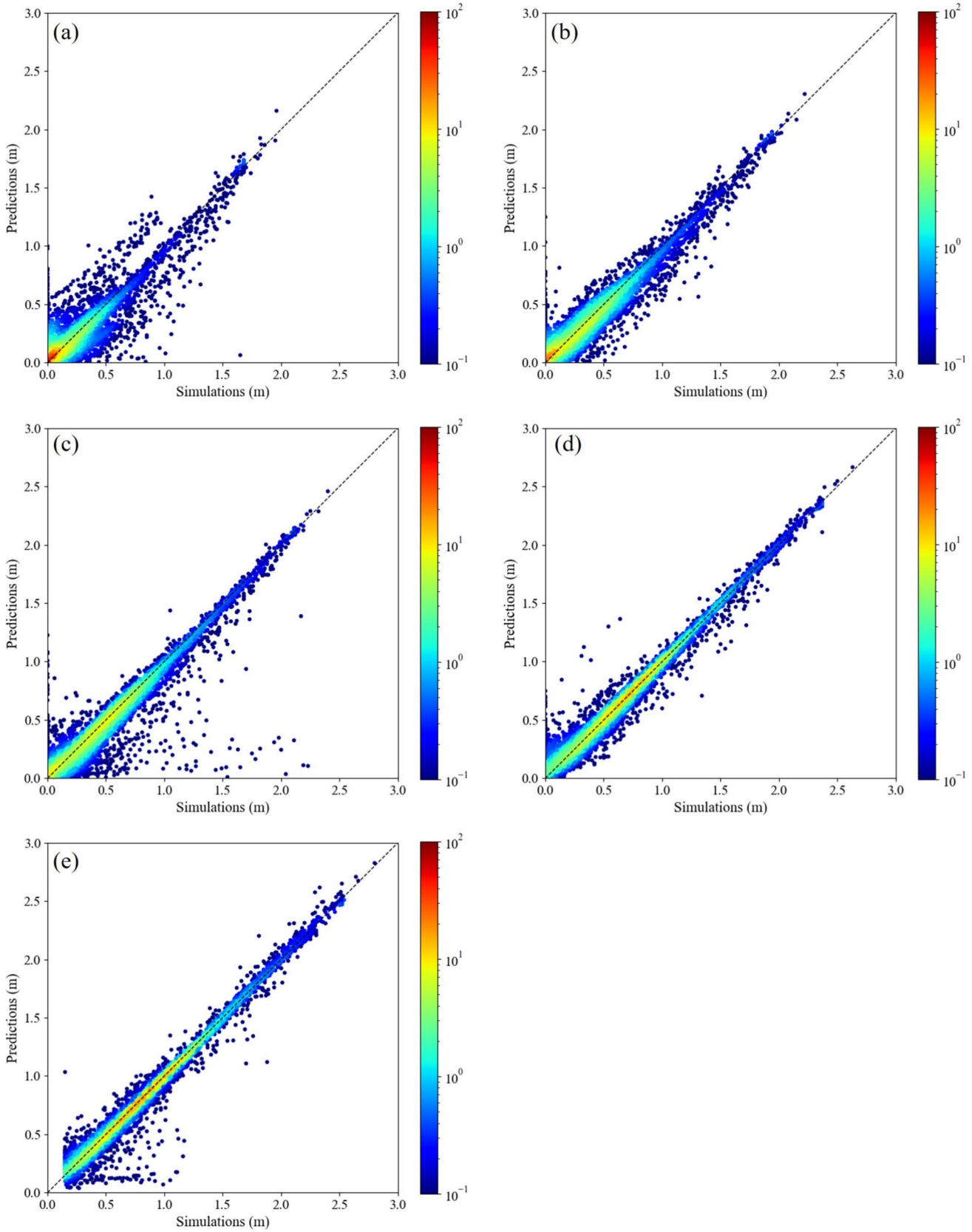
(a)
(b)
(c)
(d)
(e)
Predictions (m)
Simulations (m)
0.0
0.5
1.0
1.5
2.0
2.5
3.0
10^{2}
10^{1}
10^{0}
10^{-1}

◂**Fig. 10** Comparison between inundation depths predicted by particle swarm optimization-attention mechanism-convolutional neural network (PSO-AM-CNN) and that simulated by the Personal Computer Storm Water Management Model (PCSWMM) under **a** R5-T5, **b** R10-T10, **c** R20-T20, **d** R50-T50, **e** R100-T100 events

vertically, as the rainfall-tide level increase, the accuracy of all three models improves to some degree, and the average value of errors continues to decrease. This improvement in model accuracy is particularly significant under the R50-T50 and R100-T100. When comparing the three models horizontally, under the conditions of R5-T5, R10-T10, and R20-T20, the PSO-AM-CNN model exhibits slightly smaller errors compared to the CNN and AM-CNN models. Under R50-T50 and R100-T100, the error of depth predicted by AM-CNN is noticeably smaller than that predicted by the CNN model, while the error of depth predicted by the PSO-AM-CNN model is even smaller, with the majority of errors within 0.03 m. These findings confirm that the PSO-AM-CNN model is more advantageous in predicting inundation under worse rainfall-tide level conditions.

4.6 Interpretability Analysis of the Influence of Attention Mechanism and Hyperparameter Optimization

Shapley additive explanation analysis measures the influence of each variable value and identifies their relative importance in the model. This study used shap.DeepExplainer for model interpretability, where the training data serves as the background. The DeepExplainer implicitly samples different feature subsets through a backpropagation-based approximation, rather than explicitly enumerating all possible feature combinations. This approach efficiently estimates the marginal contribution of each feature to the model's prediction by randomly selecting feature subsets from the background data. Meanwhile, with sufficient computational resources, this study computed the SHAP values using all samples in the test dataset to ensure that the feature importance estimation fully reflects the overall prediction behavior of the model without introducing sampling bias.

Figure 13 shows the scatter plot of the importance of different features to the PSO-AM-CNN model. The results indicate that DEM is the most influential indicator affecting the model output, with its SHAP value distribution being significantly wider than that of other indicators. The three tide level indicators also rank among the top in terms of their impact on the model. This explains why the model accuracy is higher under the condition of higher tide levels. The SHAP dependency plots of DEM is presents in Fig. 14.

Table 5 Performance of the convolutional neural network (CNN), attention mechanism-CNN (AM-CNN), and particle swarm optimization-AM-CNN (PSO-AM-CNN) models

Model	MAE	RMSE	NSE
CNN	0.0689	0.1165	0.9287
AM-CNN	0.0597	0.1053	0.9418
PSO-AM-CNN	0.0528	0.0973	0.9503

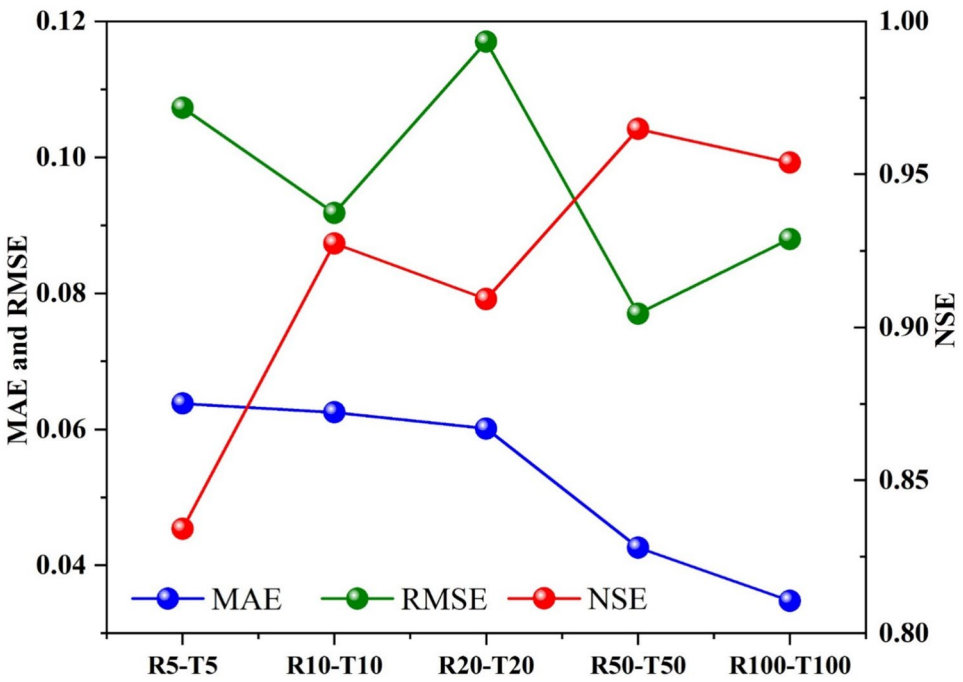

Fig. 11 Trends of the mean absolute error (MAE), root mean square error (RMSE), and Nash–Sutcliffe efficiency (NSE) values for flood prediction across different return periods

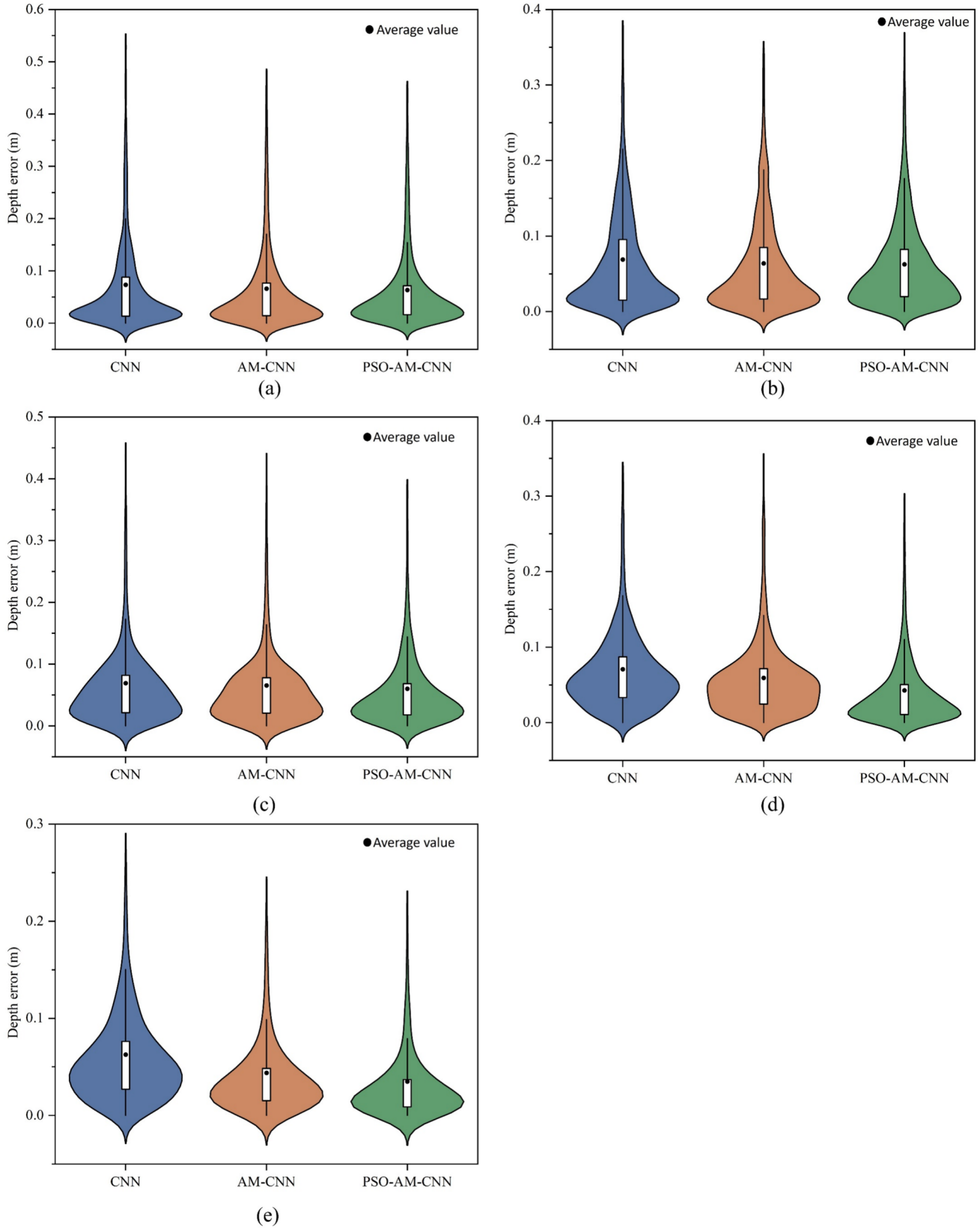

Fig. 12 The error of depth predicted by the convolutional neural network (CNN), attention mechanism-CNN (AM-CNN), and particle swarm optimization-AM-CNN (PSO-AM-CNN) models under **a** R5-T5; **b** R10-T10; **c** R20-T20; **d** R50-T50; **e** R100-T100

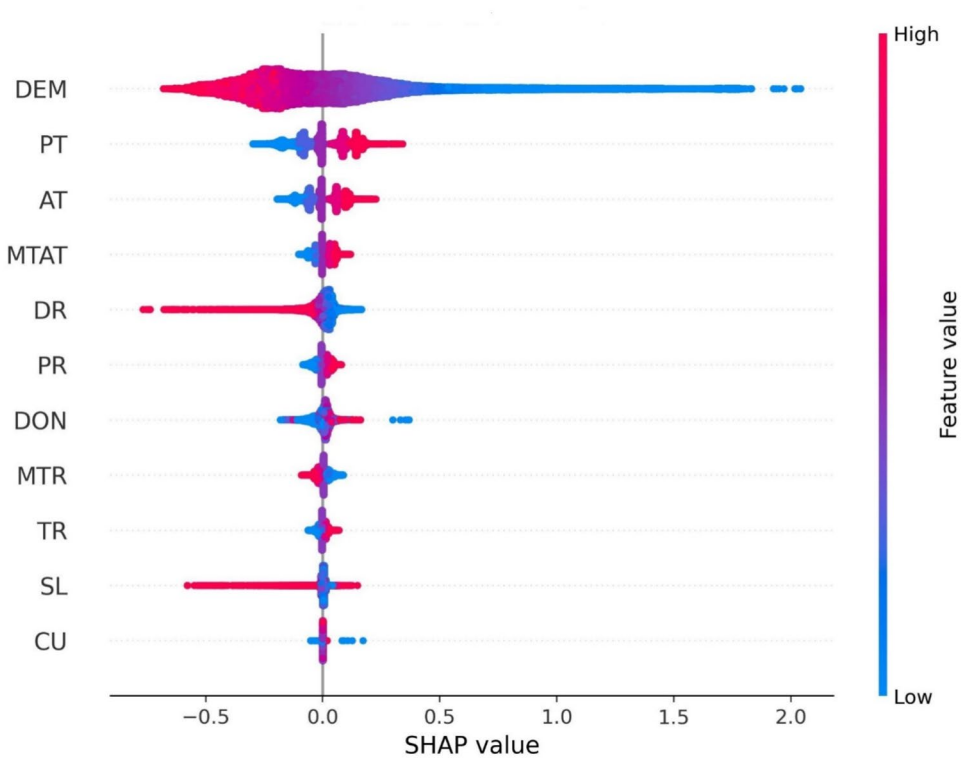

Fig. 13 Scatter plot of feature importance in the particle swarm optimization-attention mechanism-convolutional neural network (PSO-AM-CNN) model. See Table 3 for indicator names

As shown in the figure, lower DEM has a greater impact on flooding, and as DEM increases, its effect on flooding also changes. The turning point between the positive and negative effects of DEM on flooding is approximately 2.5 m. Areas with DEM below 2.5 m tend to accumulate floodwater, while those above 2.5 m show the opposite trend. Table 6 shows the variation in the model's NSE as the cumulative contribution of the DEM and tide level indicators gradually increases. From the table we can see that as the weight of important indicators increases, the model's accuracy continues to improve.

Figure 15 demonstrates the average absolute SHAP values of each input indicator in different models—higher average value indicates greater importance of the indicator in the deep learning model. From this figure, DEM and tide levels (PT, AT, and MTAT) are the most influential variables in all three models, which fully indicates that they are the most influential indicators affecting the inundation of Haidian Island. After incorporating the attention mechanism, the model pays more attention to the DEM, distance to river (DR), and tide level (PT, AT, and MTAT) indicators, increasing the weights of important flood-inducing indicator, while the model ignores the slope (SL), density of pipe network (DON), and curvature indicators (CU), reducing the weights of insignificant ones, thereby enhancing the model's accuracy. As for the rainfall indicators (TR, PR, and MTR), their weights remain small in both the AM-CNN and CNN models. After hyperparameter optimization, the structure of the model becomes more complex, the model can learn more effectively and avoid underfitting. In the PSO-AM-CNN model, while DEM and tide levels (PT, AT, and MTAT) are still the most heavily weighted indicators, the weight distribution across all indicators becomes more balanced after sufficient learning. The improved accuracy of the PSO-AM-CNN model can be attributed to its recognition of rainfall, which were not adequately considered in the previous two models.

4.7 Limitations and Future Work

This study proposed an interpretable attention mechanism-deep learning model to predict urban flooding. This model can predict urban floods quickly and accurately, and enable interpretability analysis of the deep learning. However, there are also some limitations.

Although the model was developed using data from the Haidian Island area, its framework is generalizable. In future work, for diverse terrains, the number of filters and learning rate can be adjusted accordingly to capture various hydrological response scales (for example, rapid runoff in mountainous cities versus slower surface flow in plain areas). For different climate zones, input indicators such as evapotranspiration, soil moisture, or seasonal rainfall indices can be incorporated, to enable model transferability across humid and semi-arid regions. These strategies would enhance the robustness and scalability of the proposed model.

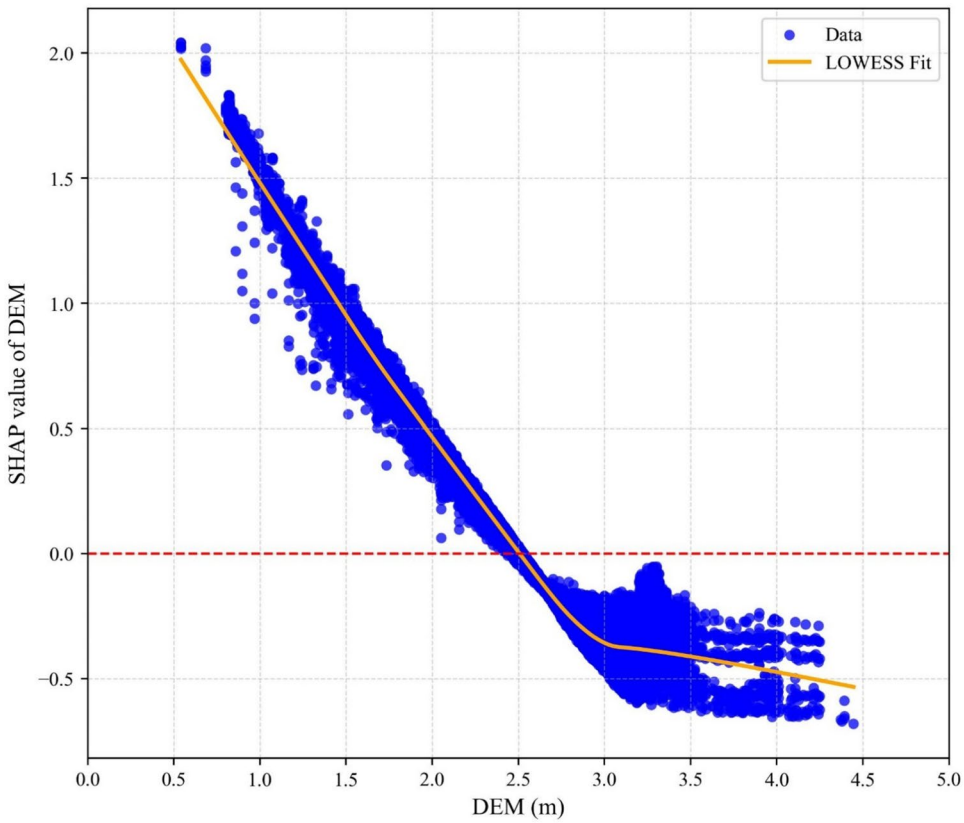

Fig. 14 Shapley additive explanation (SHAP) dependency plots of the digital elevation model (DEM)

Table 6 Variation of Nash-Sutcliffe efficiency (NSE) as the proportion of cumulative contribution of the digital elevation model (DEM) and tide level indicators gradually increases

Proportion	15%	25%	35%	45%	55%	65%	75%	85%
NSE	0.5556	0.5711	0.6984	0.7305	0.7789	0.8514	0.9259	0.9568

The model developed in this study performs well in the current research area, but when applied to other cities, it may require reconstructing the convolutional neural network and re-optimizing the hyperparameters to achieve the best predictive performance. Future research could consider transfer learning techniques (Ayana et al. 2021) to lower the cost of developing deep learning models for different cities. In addition, the model was trained and validated for flood events up to the 100-year return period; however, its predictive stability under extreme low-probability flood events (for example, with a 200-year return period) remains uncertain. The model achieved good performance in predicting inundation under long-sequence rainfall-tide conditions; however, its performance may decline when faced with insufficient data (such as short-duration rainfall time series). Future work could consider incorporating more extreme flood events into the database and applying data augmentation techniques to address the problem of insufficient data.

5 Conclusion

Urban flooding has become one of the major global disasters, and revealing the impact of weight changes of different flood-inducing factors on model accuracy is of great significance for exploring the underlying logic of deep learning models and guiding flood control and drainage efforts. This study developed an urban flood prediction model based on deep learning combining attention mechanism and interpretability analysis. In this study, CNN was used to predict the flooding situation of Haidian Island. In order to improve the model's focus on critical flood-inducing factors and improve prediction accuracy, we added the attention mechanism into deep learning model, which increases the model's NSE from

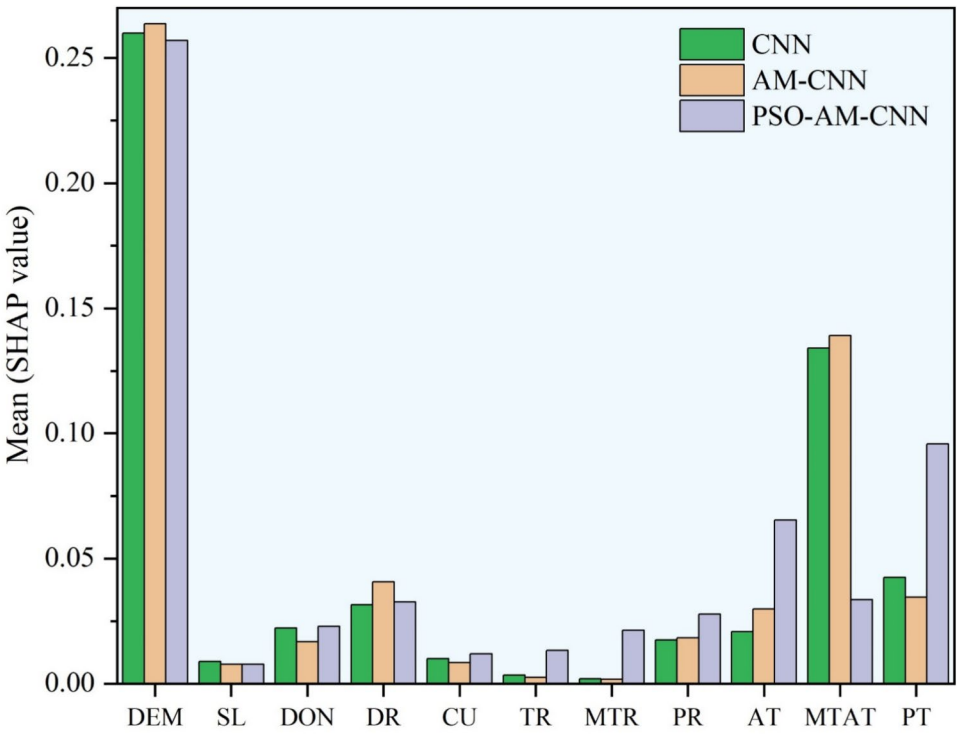

Fig. 15 Average absolute Shapley additive explanation (SHAP) values of each input indicator in different models. See Table 3 for indicator names

0.9287 to 0.9418. Particle swarm optimization was adopted for optimizing the hyperparameters in the model. After 100 iterations, suitable hyperparameters were identified, resulting in an increase of the NSE to 0.9503. This study used SHAP to analyze the interpretability of different models. The AM-CNN model increases the weights of key indicators, including DEM, distance to river, and tide level; in the PSO-AM-CNN model, the learning process becomes more comprehensive, increasing the weights of the rainfall indicators that were overlooked by the unoptimized model. The developed interpretable deep learning model can effectively predict urban flooding and support the sustainable development of cities.

Acknowledgments This study was supported by the National Natural Science Foundation of China (Grant No. 52579025), National Key R&D Program of China (Grant No. 2022YFC3090601–4), Excellent Youth Foundation of Henan Scientific Committee (Grant No. 242300421038), Scientific and Technological Projects of Henan Province (Grant No. 252102321020), Young Elite Scientists Sponsorship Program by HAST (Grant No. 2025HYTP031), and National Natural Science Foundation of China (Grant No. 52109040).

References

Ali, Y.A., E.M. Awwad, M. Al-Razgan, and A. Maarouf. 2023. Hyperparameter search for machine learning algorithms for optimizing the computational complexity. *Processes* 11(2): Article 349.

Alizadeh, B., A. Ghaderi Bafti, H. Kamangir, Y. Zhang, D.B. Wright, and K.J. Franz. 2021. A novel attention-based LSTM cell post-processor coupled with Bayesian optimization for streamflow prediction. *Journal of Hydrology* 601: Article 126526.

Ayana, G., K. Dese, and S.-W. Choe. 2021. Transfer learning in breast cancer diagnoses via ultrasound imaging. *Cancers* 13(4): Article 738.

Bass, B., and P. Bedient. 2018. Surrogate modeling of joint flood risk across coastal watersheds. *Journal of Hydrology* 558: 159–173.

Bouktif, S., A. Fiaz, A. Ouni, and M.A. Serhani. 2018. Optimal deep learning LSTM model for electric load forecasting using feature selection and genetic algorithm: Comparison with machine learning approaches. *Energies* 11(7): Article 1636.

Brauwers, G., and F. Frasincar. 2023. A general survey on attention mechanisms in deep learning. *IEEE Transactions on Knowledge and Data Engineering* 35(4): 3279–3298.

Britz, D., A. Goldie, M.-T. Luong, and Q. Le. 2017. Massive exploration of neural machine translation architectures. *Proceedings of the 2017 Conference on Empirical Methods in Natural Language Processing*, 7–11 September 2017, Copenhagen, Denmark, 1442–1451.

Cheng, L., Z. Wang, R. Pei, and J. Wu. 2025. Sustainable urban management and flood resilience in China's Yangtze River Economic Belt: Drivers, patterns, and policy synergies. *Sustainable Cities and Society* 131: Article 106737.

Gao, W., Y. Liao, Y. Chen, C. Lai, S. He, and Z. Wang. 2024. Enhancing transparency in data-driven urban pluvial flood prediction using an explainable CNN model. *Journal of Hydrology* 645(Part A): Article 132228.

Guo, M.-H., Z.-N. Liu, T.-J. Mu, and S.-M. Hu. 2023. Beyond self-attention: External attention using two linear layers for visual tasks. *IEEE Transactions on Pattern Analysis and Machine Intelligence* 45(5): Article 5436.

Hemel, R.I., and S. Sakib. 2024. Flood prediction in Bangladesh using machine learning and explainable AI: A comparative study. In *Proceedings of the 27th International Conference on Computer and Information Technology (ICCIT)*, 20–22 December 2024, Cox's Bazar, Bangladesh, 616–621.

Huang, H., Z. Wang, Y. Liao, W. Gao, C. Lai, X. Wu, and Z. Zeng. 2024. Improving the explainability of CNN-LSTM-based flood prediction with integrating SHAP technique. *Ecological Informatics* 84: Article 102904.

Kabir, S., S. Patidar, X. Xia, Q. Liang, J. Neal, and G. Pender. 2020. A deep convolutional neural network model for rapid prediction of fluvial flood inundation. *Journal of Hydrology* 590: Article 125481.

Kang, N., Z. Wang, A. Zhang, and H. Chen. 2025. Improving the prediction of streamflow in large watersheds based on seasonal trend decomposition and vectorized deep learning models. *Ecological Informatics* 90: Article 103291.

LeCun, Y., B. Boser, J.S. Denker, D. Henderson, R.E. Howard, and W. Hubbard. 1989. Backpropagation applied to handwritten zip code recognition. *Neural Computation* 1(4): 541–551.

Li, Y., F.B. Osei, S. Dai, T. Hu, and A. Stein. 2025. Identifying landscape patterns at different scales as driving factors for urban flooding. *Ecological Indicators* 176: Article 113614.

Liu, S., X. Ma, H. Wu, and Y. Li. 2020. An end to end framework with adaptive spatio-temporal attention module for human action recognition. *IEEE Access* 8: 47220–47231.

Liu, J., T. Song, C. Mei, H. Wang, D. Zhang, and S. Nazli. 2024. Flood risk zoning of cascade reservoir dam break based on a 1D-2D coupled hydrodynamic model: A case study on the Jinsha-Yalong River. *Journal of Hydrology* 639: Article 131555.

Lundberg, S.M., and S.-I. Lee. 2017. A unified approach to interpreting model predictions. *Proceedings of the 31st International Conference on Neural Information Processing Systems (NIPS'17)*, 2–6 December 2024, 4768–4777.

Lv, H., J. Chen, T. Pan, T. Zhang, Y. Feng, and S. Liu. 2022. Attention mechanism in intelligent fault diagnosis of machinery: A review of technique and application. *Measurement* 199: Article 111594.

Ma, C., Z. Chen, K. Zhao, H. Xu, and W. Qi. 2022. Improved urban flood risk assessment based on spontaneous-triggered risk assessment conceptual model considering road environment. *Journal of Hydrology* 608: Article 127693.

Ma, B., Z. Wu, C. Hu, H. Wang, H. Xu, D. Yan, and S.-e.-h. Soomro. 2022. Process-oriented SWMM real-time correction and urban flood dynamic simulation. *Journal of Hydrology* 605: Article 127269.

Manchikatla, S.K., and N.V. Umamahesh. 2022. Simulation of flood hazard, prioritization of critical sub-catchments, and resilience study in an urban setting using PCSWMM: A case study. *Water Policy* 24(8): 1247–1268.

Mei, C., H. Shi, J. Liu, T. Song, J. Wang, X. Gao, H. Wang, and M. Li. 2024. Analyzing urban form influence on pluvial flooding via numerical experiments using random slices of actual city data. *Journal of Hydrology* 633: Article 130916.

Nash, J.E., and J.V. Sutcliffe. 1970. River flow forecasting through conceptual models part I – A discussion of principles. *Journal of Hydrology* 10(3): 282–290.

Niu, Z., G. Zhong, and H. Yu. 2021. A review on the attention mechanism of deep learning. *Neurocomputing* 452: 48–62.

Pan, S., Z. Zheng, Z. Guo, and H. Luo. 2022. An optimized XGBoost method for predicting reservoir porosity using petrophysical logs. *Journal of Petroleum Science and Engineering* 208(Part C): Article 109520.

Park, J., W.H. Lee, K.T. Kim, C.Y. Park, S. Lee, and T.-Y. Heo. 2022. Interpretation of ensemble learning to predict water quality using explainable artificial intelligence. *Science of the Total Environment* 832: Article 155070.

Pradhan, B., S. Lee, A. Dikshit, and H. Kim. 2023. Spatial flood susceptibility mapping using an explainable artificial intelligence (XAI) model. *Geoscience Frontiers* 14(6): Article 101625.

Ribalta Lorenzo, P., J. Nalepa, M. Kawulok, L. Sanchez Ramos, and J.R. Pastor. 2017. Particle swarm optimization for hyper-parameter selection in deep neural networks. *Proceedings of the Genetic and Evolutionary Computation Conference* GECCO'17, 15–19 July 2017, New York, USA, 481–488.

Tang, J., G. Liu, and Q. Pan. 2021. A review on representative swarm intelligence algorithms for solving optimization problems: Applications and trends. *IEEE/CAA Journal of Automatica Sinica* 8(10): 1627–1643.

Tani, L., D. Rand, C. Veelken, and M. Kadastik. 2021. Evolutionary algorithms for hyperparameter optimization in machine learning for application in high energy physics. *The European Physical Journal C* 81(2): Article 170.

Wang, H., S. Xu, H. Xu, Z. Wu, T. Wang, and C. Ma. 2023. Rapid prediction of urban flood based on disaster-breeding environment clustering and Bayesian optimized deep learning model in the coastal city. *Sustainable Cities and Society* 99: Article 104898.

Wang, Z., N. Xu, X. Bao, J. Wu, and X. Cui. 2024. Spatio-temporal deep learning model for accurate streamflow prediction with multi-source data fusion. *Environmental Modelling & Software* 178: Article 106091.

Wu, J., Z. Wang, J. Dong, Z. Yao, X. Chen, and H. Fan. 2024. Multi-step ahead dissolved oxygen concentration prediction based on knowledge guided ensemble learning and explainable artificial intelligence. *Journal of Hydrology* 636: Article 131297.

Wu, Z., W. Xue, H. Xu, D. Yan, H. Wang, and W. Qi. 2022. Urban flood risk assessment in Zhengzhou, China, based on a D-number-improved analytic hierarchy process and a self-organizing map algorithm. *Remote Sensing* 14(19): Article 4777.

Xu, K., Z. Han, H. Xu, and L. Bin. 2023. Rapid prediction model for urban floods based on a light gradient boosting machine approach and hydrological-hydraulic model. *International Journal of Disaster Risk Science* 14(1): 79–97.

Xu, Y., C. Hu, Q. Wu, S. Jian, Z. Li, Y. Chen, G. Zhang, Z. Zhang, and S. Wang. 2022. Research on particle swarm optimization in LSTM neural networks for rainfall-runoff simulation. *Journal of Hydrology* 608: Article 127553.

Xu, H., C. Ma, J. Lian, K. Xu, and E. Chaima. 2018. Urban flooding risk assessment based on an integrated k-means cluster algorithm and improved entropy weight method in the region of Haikou, China. *Journal of Hydrology* 563: 975–986.

Xu, H., C. Ma, K. Xu, J. Lian, and Y. Long. 2020. Staged optimization of urban drainage systems considering climate change and hydrological model uncertainty. *Journal of Hydrology* 587: Article 124959.

Xue, W., Z. Wu, H. Xu, H. Wang, C. Ma, and Y. Zhou. 2024. A framework for amplification flood risk assessment and threshold determination of combined rainfall and river level in an inland city. *Journal of Hydrology* 640: Article 131725.

Yan, X., K. Xu, W. Feng, and J. Chen. 2021. A rapid prediction model of urban flood inundation in a high-risk area coupling machine learning and numerical simulation approaches. *International Journal of Disaster Risk Science* 12(6): 903–918.

Yang, L., and A. Shami. 2020. On hyperparameter optimization of machine learning algorithms: Theory and practice. *Neurocomputing* 415: 295–316.

Yang, J., K. Liu, M. Wang, G. Zhao, W. Wu, and Q. Yue. 2024. A convolutional neural network-weighted cellular automaton model for the fast prediction of urban pluvial flooding processes. *International Journal of Disaster Risk Science* 15(1): 754–768.

Yao, Z., Z. Wang, D. Wang, J. Wu, and L. Chen. 2023. An ensemble CNN-LSTM and GRU adaptive weighting model based improved sparrow search algorithm for predicting runoff using historical meteorological and runoff data as input. *Journal of Hydrology* 625(Part A): Article 129977.

Zhang, Y., C. Li, H. Duan, K. Yan, J. Wang, and W. Wang. 2023. Deep learning based data-driven model for detecting time-delay water quality indicators of wastewater treatment plant influent. *Chemical Engineering Journal* 467: Article 143483.

Zhang, X., Z. Wu, H. Wang, C. He, F. Zhang, and Y. Zhou. 2024. Urban meteorological drought comprehensive index based on a composite fuzzy matter element-moment estimation weighting model. *iScience* 27(9): Article 110798.

Zhu, X., H. Guo, and J.J. Huang. 2024. Urban flood susceptibility mapping using remote sensing, social sensing and an ensemble machine learning model. *Sustainable Cities and Society* 108: Article 105508.